Marine Pollution Bulletin 209 (2024) 117081

Contents lists available at ScienceDirect

Marine Pollution Bulletin

journal homepage: www.elsevier.com/locate/marpolbul

Effect-directed analysis and nontarget screening for identifying AhR-active substances in sediments of Gamcheon Harbor, South Korea

Jiyun Gwak [a], Junghyun Lee [b], Jihyun Cha [a], Hyo-Bang Moon [c], Jong Seong Khim [d,*], Seongjin Hong [a,*]

[a] Department of Earth, Environmental & Space Sciences, Chungnam National University, Daejeon 34134, Republic of Korea
[b] Department of Environmental Education, Kongju National University, Gongju 32588, Republic of Korea
[c] Department of Marine Science and Convergence Engineering, Hanyang University, Ansan 15588, Republic of Korea
[d] School of Earth and Environmental Sciences & Research Institute of Oceanography, Seoul National University, Seoul 08826, Republic of Korea

ARTICLE INFO

Keywords:
H4IIE-*luc* bioassay
Dioxin-like compounds
Nontarget screening
Sediment
Chemicals of concern

ABSTRACT

Gamcheon Harbor in Busan, the largest port city in South Korea, is contaminated with persistent toxic substances, including polycyclic aromatic hydrocarbons (92 to 1700 ng g^{-1} dry mass (dm)) and styrene oligomers (17 to 520 ng g^{-1} dm). This study applied effect-directed analysis and nontarget screening (NTS) to identify aryl hydrocarbon receptor (AhR)-active substances in Gamcheon harbor sediments. Relatively great AhR-mediated potencies were found in RP-HPLC fractions, F2.7–F2.8 (mid-polar, log K_{OW} 6–8) and F3.6–F3.7 (polar, log K_{OW} 5–7). Target AhR agonists comprised up to 43% of total AhR-mediated potencies. NTS using GC-QTOFMS and LC-QTOFMS identified daphnoretin and isorhamnetin as significant AhR agonists, with relative potency values of 0.4×10^{-3} and 6.5×10^{-5}, respectively, compared to benzo[*a*]pyrene. The major AhR agonists in the coastal sediments of Korea appeared to be region-specific. This approach is useful for identifying and managing key toxic substances in coastal ecosystems.

1. Introduction

Persistent toxic substances (PTSs), primarily sourced from industrial activities, enter the coastal environment and accumulate in sediments through biogeochemical processes (Hong et al., 2012). Among PTSs, polycyclic aromatic hydrocarbons (PAHs) and styrene oligomers (SOs) are prevalent in coastal sediments adjacent to industrial complexes in South Korea, with their composition varies based on the type of industrial activity (Hong et al., 2019; Lee and Khim, 2022). PTSs in sediments do not decompose easily, can cause toxicity to living organisms, and may accumulate in their bodies (Zhao et al., 2021). Previous studies have shown that some PAHs and SOs can bind to aryl hydrocarbon receptors (AhR), potentially triggering carcinogenic and developmental effects in marine organisms (Eichbaum et al., 2014; Hong et al., 2016a; Mimura and Fujii-Kariyama, 2003; Xiao et al., 2017). Thus, the characterization of AhR agonists in sediments is crucial due to their potential adverse effects on marine life.

Effect-directed analysis (EDA) has been employed for several years to identify major causative toxicants in environment samples. In previous studies, EDA was successfully applied with multi-step fractionation to reduce sample complexity and evaluate the contribution of chemicals analyzed through target chemical analysis (Hong et al., 2016b; Jeon et al., 2017). However, the presence of various environmental chemicals poses challenges to this approach. To overcome these challenges, EDA combined with nontarget screening (NTS) was developed (Zwart et al., 2020). NTS is a promising method for identifying unknown or unmonitored toxicants in the environment because it enables precise mass detection using high-resolution mass spectrometry, including quadrupole-time-of-flight mass spectrometry (QTOFMS) (Ibáñez et al., 2008; Schymanski et al., 2015).

Recent advancements have successfully identified novel AhR agonists in coastal sediments from South Korea using EDA combined with NTS (Cha et al., 2019; Kim et al., 2019; Lee et al., 2020; Gwak et al., 2022). Most previous studies have focused on the identification of mid-polar AhR agonists. However, AhR binding affinity has been observed not only in mid-polar agonists but also in polar AhR agonists. Recently, studies have been conducted to identify AhR agonists in the polar fractions of coastal sediments in South Korea (Cha et al., 2021).

* Corresponding authors.
E-mail addresses: jskocean@snu.ac.kr (J.S. Khim), hongseongjin@cnu.ac.kr (S. Hong).

https://doi.org/10.1016/j.marpolbul.2024.117081
Received 18 July 2024; Received in revised form 27 September 2024; Accepted 30 September 2024
Available online 10 October 2024

Nevertheless, polar AhR agonists have shown a very low contribution to AhR-mediated potencies compared to mid-polar agonists. To further determine the relative contribution of the polar fraction, studies should be performed to identify unknown or unmonitored polar AhR agonists in environmental samples.

Gamcheon Harbor in Busan City is the largest port area in South Korea, encompassing various industrial zones, including factories and shipyards, along the coastline (Hong et al., 2005; Moon et al., 2007). Monitoring of tributyltin, an antifouling agent, was conducted in a previous study, but the investigation into PAHs and SOs was limited (Lee and Khim, 2022). As a designated "Specially-Managed Sea Area (SMSA)," the Busan Coast is subject to close scrutiny due to the high pollution load from nearby industries and various human activities. However, studies on AhR-mediated potencies in sediments have been limited. AhR-active substances from multiple anthropogenic activities around Gamcheon Harbor can be introduced into the environment and may accumulate in the harbor sediments.

The research hypothesis of the present study is that unmonitored AhR-active substances exist in the sediment samples from Gamcheon Harbor. This study aims to evaluate the contamination status of Gamcheon Harbor sediments through target chemical analysis and in vitro bioassays and to identify previously unmonitored toxicants by conducting EDA on highly toxic sediment extracts. The specific objectives were: (i) to investigate the concentrations of mid-polar and polar AhR agonists in sediments, (ii) to assess AhR-mediated potencies using H4IIE-*luc* bioassays, (iii) to identify unmonitored AhR-active compounds in highly potent fractions through nontarget screening, (iv) to determine the relative contribution of individual compounds through potency balance analysis, and (v) to compare the major AhR agonists observed in this study with those from previous studies conducted in Korean coastal waters.

2. Materials and methods

2.1. Sample collection and preparation

Gamcheon Harbor is characterized by a variety of anthropogenic activities, including a container yard, building material yard, ship repair pier, seafood storage facilities, LPG power plant, and fish market (Fig. 1a). Since the establishment of Busan New Harbor, Gamcheon Harbor has experienced a rapid decline in cargo volume, particularly in container handling. Despite this, this area is well-known for its abundant marine life due to its deep waters and favorable currents. In May 2019, surface sediment samples were collected from 12 sites (S1–S12) (Fig. 1a). These sites were chosen to assess the impact of various anthropogenic activities around Gamcheon Harbor, as previously mentioned. The sampling sites in this study were selected in a manner similar to previous studies (Choi et al., 2010; Moon et al., 2007), which investigated sediment contamination by tributyltin and polybrominated diphenyl ethers at comparable sites. These samples were placed in glass bottles, stored in ice boxes, and kept frozen at –20 °C upon arrival at the laboratory until further analysis. The sediment samples were then freeze-dried, sieved through a 1-mm mesh, and homogenized. Forty grams of these sediments were extracted with 350 mL of dichloromethane (DCM, J.T. Baker, Phillipsburg, NJ) using a Soxhlet extractor for 16 h. Activated copper was added to the raw organic extracts (REs) for 1 h to remove sulfur. The REs were then concentrated to a final volume of 4 mL, representing 10 g of sediment (SEq) per mL, utilizing a rotary evaporator and a nitrogen concentrator. The concentrated REs were divided into two aliquots: 3 mL for silica gel fractionation and 1 mL for bioassays. The solvent in the REs allocated for bioassays was substituted with dimethyl sulfoxide (Sigma-Aldrich, St. Louis, MO).

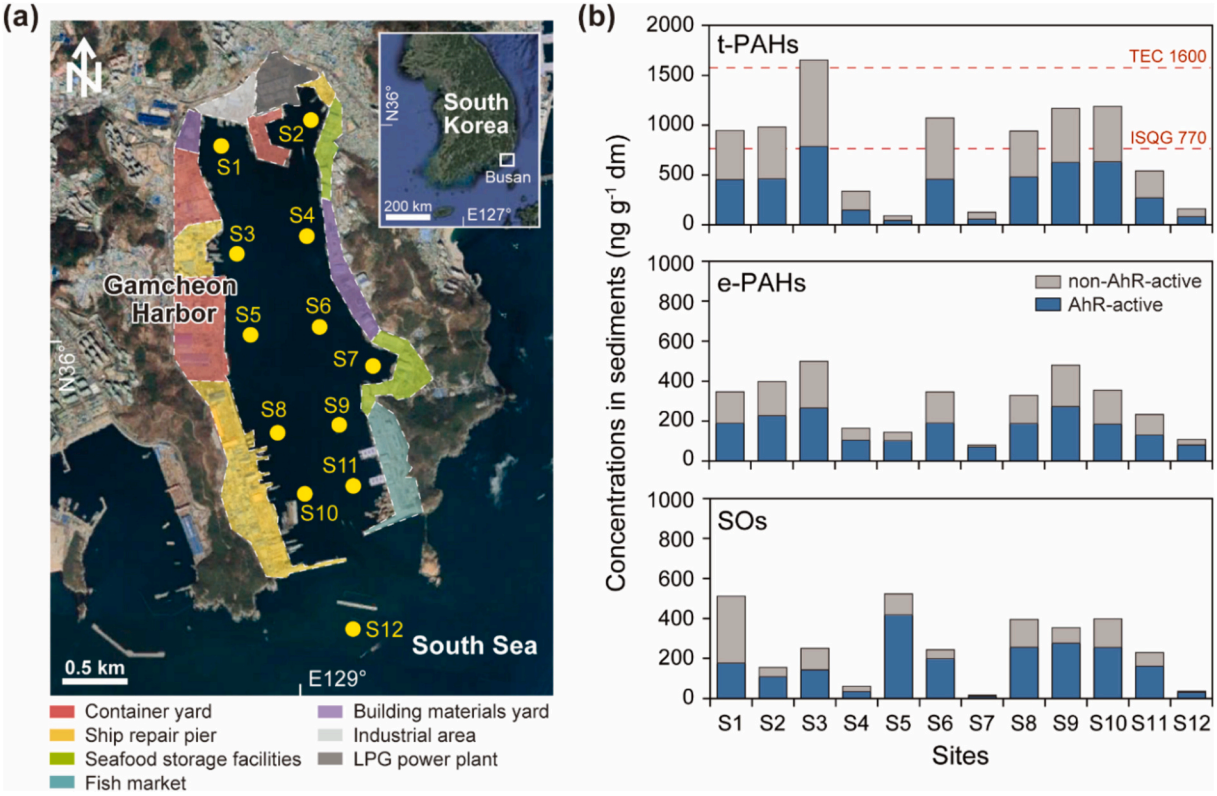

Fig. 1. (a) Map showing the sampling sites of surface sediments and local activities in Gamcheon Harbor, South Korea. (b) Concentrations of traditional PAHs (t-PAHs), emerging PAHs (e-PAHs), and styrene oligomers (SOs) of sediments in Gamcheon Harbor. The blue bar represents the concentrations of AhR-active compounds. (For interpretation of the references to color in this figure legend, the reader is referred to the web version of this article.)

2.2. Silica gel and RP-HPLC fractionations

Fractionation was performed in two steps: silica gel column chromatography and reverse-phase high-performance liquid chromatography (RP-HPLC, Agilent 1260, Agilent Technologies, Santa Clara, CA). For the silica gel fractionation, 3 mL of the REs was loaded onto a silica gel column and separated into three fractions: F1 (non-polar), F2 (mid-polar), and F3 (polar). F1, F2, and F3 were eluted with 30 mL of hexane (Honeywell, Charlotte, NC), 60 mL of hexane:DCM (8:2), and 50 mL of acetone (J.T. Baker):DCM (6:4), respectively. Previous studies have shown that F1 contains non-polar compounds such as polychlorinated biphenyls, F2 includes mid-polar compounds such as PAHs and SOs, and F3 contains polar compounds such as alkylphenols and pharmaceuticals (Kim et al., 2019; Lee et al., 2020; Cha et al., 2022). The eluted fractions were then concentrated to a final volume of 3 mL using a rotary evaporator and a nitrogen concentrator. Out of the 3 mL silica gel fraction, 1 mL was allocated for RP-HPLC fractionation. The instrumental conditions for RP-HPLC separation are provided in Table S1 of the Supplementary Materials. The fractionation conditions for RP-HPLC were previously optimized using standard materials of various model compounds, including 34 polychlorinated biphenyls, 16 PAHs, 7 alkylphenols, and 5 phthalates (Hong et al., 2016b). The same procedures were followed for the analysis of procedural blank samples.

2.3. H4IIE-luc in vitro bioassays

The AhR binding affinity in REs of the sediments, silica gel fractions, and RP-HPLC fractions were measured using H4IIE-*luc* recombinant cells. Details of cell culture and experimental procedures, including seeding, dosing, and instrumental measurements, are provided in Table S2. Exposure concentrations for the cells were established at 10 g of SEq mL^{-1}. Benzo[*a*]pyrene (BaP) was used as a positive control, effectively targeting mid-polar and polar compounds that undergo metabolism in the H4IIE-*luc* bioassay upon 4-h exposure. The bioassay response was converted into percentages of the maximum response to BaP. Luminescence measurements were conducted using a Victor multilabel plate reader (PerkinElmer, Waltham, MA). Potency-based BaP-equivalent concentrations (BaP-EQs) were derived from the dose-response curve. The dose-response curve was generated by diluting the sediment samples to six different concentrations. To ensure reproducibility, all samples were tested three times during the bioassay.

2.4. Target chemical analysis

PAHs were designated as priority pollutants by the US Environmental Protection Agency (EPA) and defined as traditional PAHs (t-PAHs) in this study. PAHs identified through EDA combined with NTS were classified as emerging PAHs (e-PAHs). The full names and method detection limits of these compounds are listed in Table S3. A total of fifteen t-PAHs, eighteen e-PAHs, and ten SOs in REs and fractions were analyzed using an Agilent 7900B gas chromatograph (GC) equipped with 5977A mass-selective detector (MSD) (Agilent Technologies) (Table S4). The column used for separation was a DB-5MS. The flow rate and injection volume were set at 1.0 mL min^{-1} and 1 μL, respectively. The mass range was 50–600 *m/z*, and the ion source temperature was 230 °C. The ionization mode used was electron ionization (EI). Isotopically labeled surrogate standards (acenaphthene-*d15*, phenanthrene-*d15*, chrysene-*d15*, and pyrene-*d15*) were added to the procedural blank, and the recovery rates ranged from 67 to 105%.

The names and method detection limits of five polar AhR agonists are presented in Table S5. The target compounds were not detected in the procedural blank samples. Quantification of polar AhR agonists was conducted using a 1290 Infinity II HPLC coupled with an Agilent 6470 triple quadrupole mass spectrometer (Agilent Technologies) (Table S6). For efficient separation, a ZORBAX Eclipse XDB-C18 column was used. The column temperature was maintained at 40 °C, the injection volume was set to 3 μL, and the flow rate was adjusted to 0.4 mL min^{-1}. The ionization mode employed was electrospray ionization (ESI) in positive mode. The ion source gas and curtain gas settings were established at 50 psi and 30 psi, respectively. Additionally, the DuoSpray Ion Source was operated in positive mode at 5500 V.

2.5. Nontarget screening analysis

NTS was conducted on RP-HPLC fractions exhibiting significant AhR-mediated potencies, using GC-QTOFMS for mid-polar fractions and LC-QTOFMS for polar fractions. Detailed instrumental conditions for GC-QTOFMS and LC-QTOFMS are provided in Tables S7 and S8, respectively. Tentative mid-polar and polar AhR agonists were selected through a four-step selection process. In the first step, all peaks in the fraction samples were identified. Second, these peaks were compared with known compounds using the NIST library and TCM Library software in the GC-QTOFMS and LC-QTOFMS, respectively. Third, compounds with library matching scores ≥70 were selected. The matching score (mass accuracy score) reflects how closely the observed mass matches the theoretically expected mass. A matching score of ≥70 has been used in previous studies for the identification of untargeted compounds in environmental samples (Cha et al., 2019; Kim et al., 2019; Lee et al., 2020; Gwak et al., 2022). Finally, compounds containing aromatic ring(s) were chosen. Among the tentative polar AhR agonists, commercially available standard materials such as triphenylbenzene, trenbolone, daphnoretin, and isorhamnetin were purchased from Sigma-Aldrich.

2.6. Toxicological confirmation and potency balance analysis

The relative potency (RePs) values of mid-polar and polar AhR agonists were evaluated using the H4IIE-*luc* bioassay, utilizing effective concentrations (ECs) corresponding to 20% of the maximum response elicited by BaP (EC_{20}). EC_{20} values for the tentative polar AhR agonists were determined from dose-response curves at six concentrations ranging from 41 to 10,000 ng mL^{-1}. The RePs of target mid-polar and polar AhR agonists are shown in Tables S9 and S10, respectively. Potency balance analysis was executed to compare instrument-derived BaP-EQs ($BaP\text{-}EQ_{chem}$) with bioassay-derived BaP-EQs ($BaP\text{-}EQ_{bio}$) for the same samples, aiming to evaluate the contribution of specific AhR agonists to the overall AhR-mediated potency. $BaP\text{-}EQ_{chem}$ was calculated as the sum of the products of concentrations and RePs for individual compounds (Eq. (1)).

$$BaP - EQ_{chem} = \sum [(\text{concentration of AhR agonist}_i) \times RePs_i] \quad (1)$$

2.7. In silico modeling using VEGA QSAR

Four tentative AhR agonists identified by NTS were screened to predict various toxicological endpoints, including skin sensitization, skin irritation, eye irritation, chromosomal aberration mode, glucocorticoid receptor (GR) activity, endocrine disruptor activity screening, hepatoxicity, androgen receptor (AR) activity, carcinogenicity, developmental toxicity, estrogen receptor (ER) activity, and thyroid receptor (TR) activity using VEGA quantitative structure–activity relationship (QSAR) (Marzo et al., 2016; Vedani et al., 2015). The open-access VEGA QSAR software (version 1.2.3) was used to predict physicochemical and human toxicity data through a similar in silico approach. This method utilizes QSAR models that correlate toxicological effects with chemical structure parameters, including various molecular descriptors (Klanovicz and Pinto, 2024; Pizzo et al., 2013).

3. Results and discussion

3.1. Assessment of sediment contamination in Gamcheon Harbor

t-PAHs, e-PAHs, and SOs were detected in all sediments of Gamcheon Harbor (Fig. 1b and Table S11). The concentrations of t-PAHs and e-PAHs in sediments ranged from 92 to 1700 ng g^{-1} dry mass (dm) with a mean of 770 ng g^{-1} dm, and from 80 to 500 ng g^{-1} dm with a mean of 290 ng g^{-1} dm, respectively. Notably, the concentrations of t-PAHs at site S3 surpassed the threshold effect concentrations (TEC) of 1600 ng g^{-1} dm, indicating potential environmental risk (CCME, 2001; Solberg et al., 2003). PAHs, primarily from ship traffic and fuel combustion, showed the highest concentration at S3, near the ship repair pier and the largest harbor (Karacık et al., 2009). Previous studies have also reported that ship repair was a major source of sediment pollution in the harbor (Yu et al., 2017). Additionally, concentrations of t-PAHs in sediments exceeded interim sediment quality guidelines (ISQG) except at sites S1, S2, S6, S8, and S10 (770 ng g^{-1} dm, ISQG) (CCME, 2001). Concentrations of SOs in sediments ranged from 17 to 520 ng g^{-1} dm, with a mean of 260 ng g^{-1} dm. The greatest concentration of SOs in sediment was observed at S5, where the container yard is located. PAHs are primarily produced from incomplete combustion processes and released into the atmosphere, while SOs are predominantly formed through the thermal decomposition of plastics and introduced into the marine environment via ocean currents (Ghosh et al., 2015; Kwon et al., 2015). Due to these distinct sources and pathways, the distribution of PAHs and SOs observed at Gamcheon Harbor exhibits site-specific.

Among the target t-PAHs, e-PAHs, and SOs, several compounds are known to have AhR binding affinity (Table S11). The concentrations of AhR-active t-PAHs, e-PAHs, and SOs in sediments at sites S1–S12 ranged from 44 to 790 ng g^{-1} dm, 72 to 290 ng g^{-1} dm, and 12 to 420 ng g^{-1} dm, respectively (Fig. 1b). Target mid-polar AhR agonists were confirmed to account for most of the concentrations of t-PAHs, e-PAHs, and SOs. It is indicated that PTSs introduced from nearby industrial facilities may have caused AhR-mediated potencies in sediments. The target polar AhR agonists were mostly undetectable across most sites (<LOD–0.28 ng g^{-1} dm) due to the limited number of target compounds and challenges posed by their high water solubility (Table S12) (Von Oepen et al., 1991). Despite their low concentrations, polar AhR agonists are particularly significant due to their pharmaceutical applications and direct relevance to human life (Cha et al., 2021). The highest levels of target polar AhR agonists were detected at S3, while none of these target polar compounds were found in the sediment at S10.

3.2. AhR-mediated potencies in sediments

AhR-mediated potencies in all REs of sediments showed >100% of % BaP_{max} (Fig. S1). AhR-mediated potencies in the silica gel fractions were very low in F1 (non-polar), whereas F2 (mid-polar) and F3 (polar) showed >100% of %BaP_{max} (Fig. S1). This result corresponds to the AhR-mediated potencies observed in silica gel fractions from prior studies (Cha et al., 2019; Kim et al., 2019; Lee et al., 2020; Gwak et al., 2022). The higher AhR-mediated potencies observed in F2 and F3, relative to the REs, could be attributed to the reduced number of AhR antagonists, which are numerous in REs (Hashmi et al., 2018, 2020). The AhR-mediated potencies of F2 and F3 were the greatest in the ship repair pier region (S3 and S10). These findings were particularly pronounced near the ship repair pier (S3 and S10), suggesting this area is a primary source of AhR agonist contamination. Additional steps were performed to identify AhR agonists using sediments of S3 and S10.

F2 and F3 of S3 and S10 exhibited relatively high AhR-mediated potencies. The second-step fractionation was performed using RP-HPLC, dividing each into 10 subfractions (F2.1–F2.10 and F3.1–F3.10) (Fig. 2a and b). F3 of S10 showed greater AhR-mediated potencies compared to S3. However, AhR-mediated potencies in subfractions of S10 were smaller than those in subfractions of S3. These results may be attributed to the masking effects of certain compounds present in F2 and F3 of S3, leading to smaller observed AhR-mediated potencies compared to those of S10 (Hashmi et al., 2018, 2020). Subfractionation of F2 and F3 from S3 likely reduced the sample complexity, potentially eliminating AhR antagonists that interfere with AhR-mediated potencies. Similarly, a previous study reported the masking effect of anti-AR agonists on the AR activity of sediment extracts after fractionation (Weiss et al., 2009). Notably, F2.7 and F2.8 in both S3 and S10 exhibited considerable AhR-mediated potencies (Fig. 2a). EC_{50} values were derived from dose-response curves for F2.6–F2.8 in S3 and S10 (Fig. 2c). Potency-based BaP-EQ (BaP-EQ_{bio}) concentrations were 1100 and 170 ng BaP-EQs g^{-1} dm in F2.7 and 2800 and 2600 BaP-EQs g^{-1} dm in F2.8 of sites S3 and S10, respectively. In F2.6 of S3 and S10, BaP-EQ_{bio} concentrations had low AhR-mediated potency; thus, EC_{50} could not be calculated.

AhR-mediated potencies in F3 of S3 and S10 were notably elevated in F3.6–F3.7 (Fig. 2b). This pattern of AhR-mediated potencies in F2 and F3 subfractions of sediments aligns with observations from other industrial areas such as Ulsan Bay (Kim et al., 2019), Lake Sihwa (Cha et al., 2019, 2021), Masan Bay (Lee et al., 2020), and Yeongil Bay (Gwak et al., 2022). This suggests that AhR agonists in sediments of industrial complexes are mainly compounds with log K_{OW} 5–8. EC_{50} values were calculated from dose-response curves for F3.6–F3.7 in S3 and S10 (Fig. 2d). BaP-EQ_{bio} concentrations were 120 and 1200 ng BaP-EQs g^{-1}

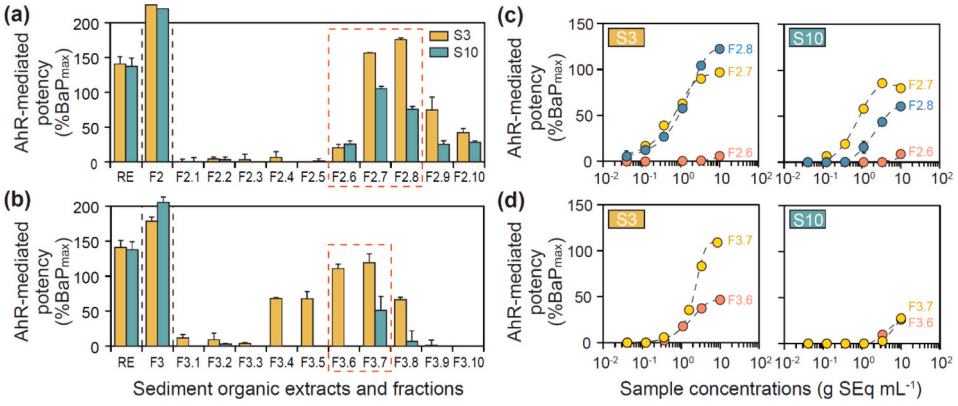

Fig. 2. AhR-mediated potencies in raw organic extracts (RE), silica gel fractions (F2: mid-polar; F3: polar), and RP-HPLC subfractions of sediments from Gamcheon Harbor, South Korea. AhR-mediated potencies of the (a) mid-polar and (b) polar fractions of S3 and S10 sediments and their RP-HPLC subfractions. Dose-response characterization for AhR-mediated potencies of selected RP-HPLC fractions, such as (c) F2.6–F2.8 and (d) F3.6–F3.7 of S3 and S10 (error bar: mean ± SD, n = 3).

dm in F3.6 and F3.7 of S3, respectively. BaP-EQ_{bio} concentrations for F3.6–F3.7 of S10 did not allow the calculation of EC_{50} due to low AhR-mediated potency. The calculated concentrations of BaP-EQ_{bio} were used in potency balance analysis.

3.3. Contribution of target mid-polar and polar AhR agonists

Concentrations of BaP-EQ_{chem} for target mid-polar AhR agonists in F2.6, F2.7, and F2.8 of S3 exhibited a range from 0.004–180 ng g^{-1} dm, 0.74–140 ng g^{-1} dm, and 68 ng g^{-1} dm, respectively. In the corresponding fractions of S10, the BaP-EQ_{chem} ranged from 0.003 to 150 ng g^{-1} dm, 0.59 to 280 ng g^{-1} dm, and 45 ng g^{-1} dm, respectively. Target mid-polar AhR agonists accounted for 22% and 2.6% of BaP-EQ_{bio} in F2.7 and F2.8 of S3, respectively (Fig. 3a), and for 43% and 26% of BaP-EQ_{bio} in F2.7 and F2.8 of S10, respectively (Fig. 3b). Specifically, in both S3 and S10, the significant contributors to F2.7 were in the following order: BaP, benzo[*j*]fluoranthene (BjF), indeno[*1,2,3-cd*]pyrene (IcdP), benzo[*b*]fluoranthene (BbF), and 10-methylbenz[*a*]pyrene (10MbA) (Table S13, Fig. 3a, and b). BaP, IcdP, and BbF are compounds produced by the incomplete combustion of coal and diesel, and they have been reported to enter sediments through ship activities, such as ship repair facilities and fuel combustion (Kado et al., 2000; Larsen and Baker, 2003; Li et al., 2016). BjF, an AhR agonist identified in sediments of Ulsan Bay through EDA combined with NTS in a previous study (Kim et al., 2019), is known to derive from pyrolysis of bituminous coal primary tar and combustion of fuel (Ledesma et al., 2000). Thus, it suggests that BaP, BjF, IcdP, and BbF were introduced via ship repair activities, influencing AhR-mediated potencies in sediments of S3 and S10.

Concentrations of BaP-EQ_{chem} for target polar AhR agonists (ciprofloxacin, genistein, mepanipyrim, protopine, and rutaecarpine) in F3 of sediments ranged from <LOD to 0.035 ng g^{-1} dm (Table S13). Most concentrations of target polar AhR agonists were below the LOD. Concentrations of BaP-EQ_{chem} in S3 and S10 were very low. This is because the RePs of target polar AhR agonists are very low (except for rutaecarpine), resulting in very low concentrations. In the potency balance analysis of F3.6 and F3.7 of S3, target polar AhR agonists accounted for only 0.3% of BaP-EQ_{bio} in F3.6, but not in F3.7 (Fig. 3c). The remaining unexplained AhR-mediated potencies might be attributed to other AhR agonists present below the LOD in this study. The fact that neither target mid-polar nor polar AhR agonists can fully explain the AhR-mediated potencies in the sediments suggests the presence of unknown and/or unmonitored AhR agonists, emphasizing the need for further identification of untargeted AhR agonists.

3.4. Identification of unmonitored AhR agonists using nontarget screening

NTS was conducted for F2.7, F2.8, F3.6, and F3.7 of S3. Tentative AhR agonists were selected through a four-step selection criterion (Cha et al., 2019; Kim et al., 2019; Lee et al., 2020; Gwak et al., 2022) (Fig. 4a). A total of 281, 294, 107, and 15 chromatographic peaks were detected in F2.7, F2.8, F3.6, and F3.7 of S3, respectively. In the second step, the number of compounds matched by NIST and TCM Library software was 138, 133, 45, and 11 in F2.7, F2.8, F3.6, and F3.7, respectively. Following this, 38, 22, 7, and 0 compounds with matching scores ≥70 were further refined (Muz et al., 2017). The final selection focused on compounds possessing aromatic ring(s), known for their binding affinity to AhR (Mekenyan et al., 1996). Consequently, four compounds were selected as tentative AhR agonist candidates. Triphenylbenzene in F2.7, along with trenbolone, daphnoretin, and isorhamnetin in F3.6, were selected as candidates for AhR agonists.

While numerous peaks were detected in environmental samples, this study identified only four compounds as tentative AhR agonist candidates. To enhance the selection of AhR agonist candidates in future studies, we propose two advanced methodologies. First, in the analysis with QTOFMS, many chromatographic peaks were identified, but more than half of the compounds were excluded during the library matching step. The library contains various compounds, including pharmaceuticals and pesticides, which can be crucial in the candidate selection process. However, there is a risk of excluding compounds that do not match the library due to the limited number of compounds, such as transformation products (TPs) (Booij et al., 2014; Hong et al., 2023; Moschet et al., 2017). Thus, it will be necessary to use additional confirmation methods, such as in silico fragmentation platforms (MS Fragementer, Mass Frontier, and MetFrag), to identify compounds not found in the library (Gago-Ferrero et al., 2015; Wolf et al., 2010). Second, the selection criteria process for active compounds can be time-consuming, and the activity of tentative compounds may not be exhibited when toxicological evaluation is performed using in vitro bioassays. Recent advancements in machine learning offer a more efficient and precise method to identify active compounds based on their toxicological profiles, as evidenced by research that successfully utilized these techniques to predict compound toxicity (Arturi and Hollender, 2023; Samanipour et al., 2022). Additionally, a recent study used deep learning to identify 12 potential AhR agonists in sediments (Cheng et al., 2024). Therefore, integrating high-throughput data analysis with machine learning could enhance the identification of compounds with unknown and strong AhR binding affinities in environmental samples.

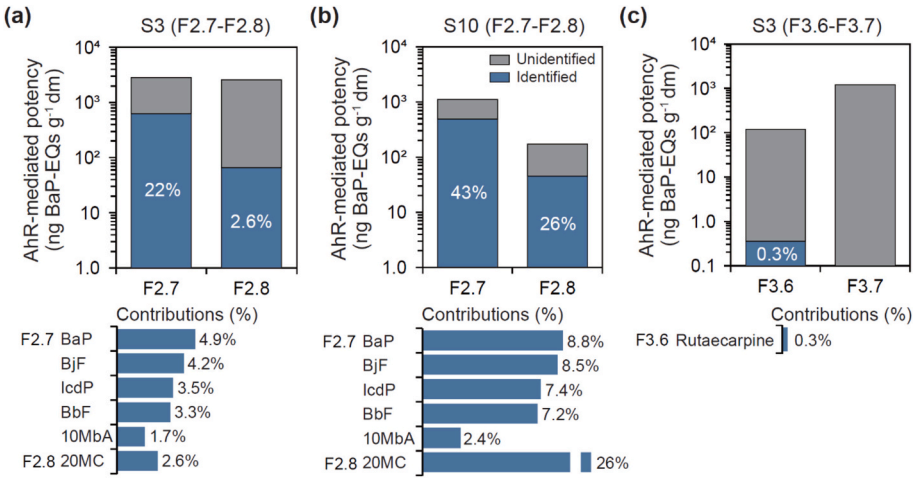

Fig. 3. Contributions of target AhR agonists (instrument-derived BaP-EQs, BaP-EQ_{chem}) to the total induced AhR-mediated potencies (bioassay-derived BaP-EQs, BaP-EQ_{bio}) of (a) F2.7 and F2.8 of S3, (b) F2.7 and F2.8 of S10, and (c) F3.6 and F3.7 of S3 (Blue bar indicates the contribution of known AhR agonist). (For interpretation of the references to color in this figure legend, the reader is referred to the web version of this article.)

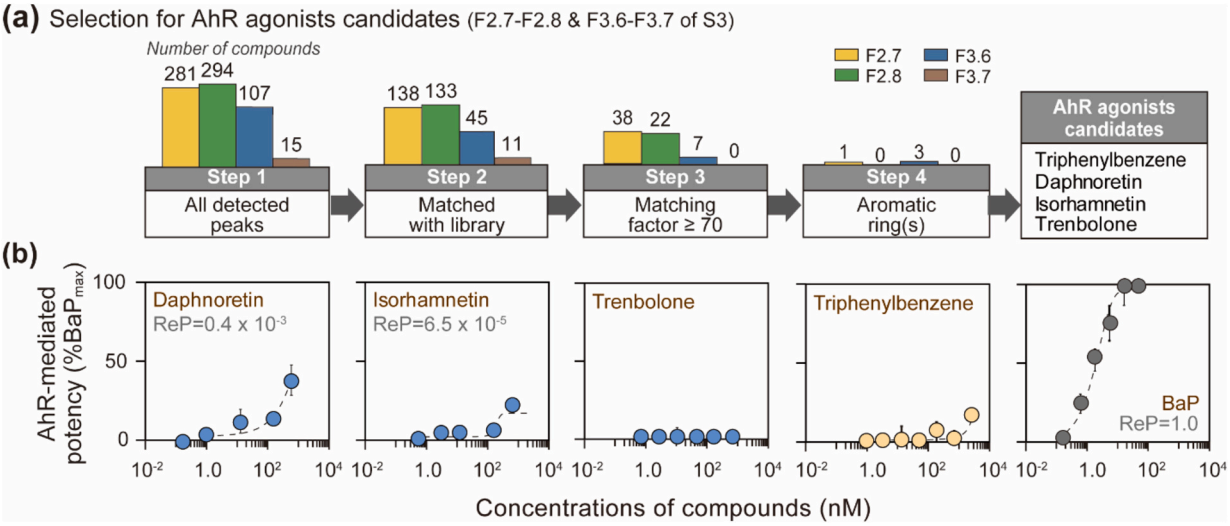

Fig. 4. (a) Nontarget screening data analysis (obtained using GC-QTOFMS for F2.6 and F2.7 of S3 and LC-QTOFMS for F3.6 and F3.7) process of AhR-active fractions for selection of AhR agonist candidates. (b) Toxicological confirmation (dose-response tests in the H4IIE-*luc* bioassay) for four tentative AhR agonists (error bar: mean ± SD, $n = 3$). Relative potency values for AhR-mediated activity of daphnoretin and isorhamnetin (i.e., newly identified AhR agonists) compared to benzo[*a*]pyrene were obtained in this study.

3.5. Toxicological and chemical confirmation

Among the selected four candidates, daphnoretin and isorhamnetin exhibited significant AhR-mediated activities (Fig. 4b). The RePs of daphnoretin and isorhamnetin were 0.4×10^{-3} and 6.5×10^{-5}, respectively, compared to BaP. This study confirmed for the first confirmation that daphnoretin can bind to AhR. Isorhamnnetin showed different results from the previous study (Kim et al., 2021). Isorhamnetin, a metabolite of quercetin, has been documented to inhibit BaP from binding to AhR (Kim et al., 2021). Exposure to a mixture of BaP and isorhamnetin in human liver cells (HepaG2) resulted in lower cytotoxicity than BaP alone. In addition, the enzyme CYP1B1, which metabolizes PAHs, increased (Kim et al., 2021). Thus, isorhamnetin, as an anti-AhR agonist, might have contributed to the antagonist effect in the fraction.

Daphnoretin and isorhamnetin, which showed AhR binding affinity, were confirmed for retention time and mass fragment ions using HPLC-MS/MS, and their concentrations in fractions were quantified (Table S14). Daphnoretin and isorhamnetin were detected only in S3 with 0.30 ng g^{-1} dm and 0.49 ng g^{-1} dm, respectively. Both daphnoretin and isorhamnetin were commonly detected in S3, where NTS was conducted. Daphnoretin originates from *Wikstroemia indica* and is used in Traditional Chinese Medicine. Isorharmnetin is a metabolite of quercetin, and quercetin has been reported as one of the flavonoids present in vegetables and fruits (Kim et al., 2021).

Daphnoretin and isorhamnetin explained only 0.0001% of AhR-mediated potency in F3.6 of S3. Both target and novel polar AhR agonists contributed a small portion to the total AhR-mediated potencies. Previous studies have identified pharmaceuticals as significant polar AhR agonists in environmental samples (Kim et al., 2021; Cha et al., 2021). Pharmaceuticals can undergo various TPs in the environment through abiotic and biotic processes (Heberer, 2002). Even after transformation, these TPs may still exhibit stronger AhR binding affinity compared to parent compounds (Escher and Fenner, 2011). However, identifying TPs can be challenging, as they could not identified during NTS due to the lack of libraries. Thus, further efforts to identify polar AhR-active substances, including TPs, will be necessary in future research.

3.6. Predictions of additional potential toxicity

VEGA QSAR was utilized to predict additional toxicities for the four AhR agonist candidates. These toxicities encompassed GR activity, AR activity, ER activity TR activity, skin sensitization, skin irritation, eye irritation, chromosomal aberration, endocrine disruptor activity screening, hepatoxicity, carcinogenicity, and developmental toxicity (Table 1). Triphenylbenzene was predicted to exhibit skin sensitization, developmental toxicity, ER activity, and mutagenicity. Daphnoretin and isorhamnetin were predicted to have all potential toxicities except TR, hepatoxicity, and endocrine disruptor activity screening. The toxicity of daphnoretin and isorhamnetin, which showed significant AhR-mediated potencies in this study, was previously predicted using VirtualToxLab (Cha et al., 2022). The results indicated that daphnoretin has a binding affinity to AR. The prediction of the three compounds using the CompTox chemistry dashboard indicated that triphenylbenzene and isorhamnetin have ER binding affinity. These results indicate that the identified compounds, mainly originating from local activities around the harbor, have the potential to induce a range of toxic effects on the environment and pose risks to human health.

3.7. Comparison of major AhR agonists in sediments of Korean coastal waters

In previous studies conducted in various industrial complexes across Korean coastal waters, including Ulsan Bay (Kim et al., 2019), Lake Sihwa (Cha et al., 2019, 2021), Masan Bay (Lee et al., 2020), and Yeongil Bay (Gwak et al., 2022), EDA combined with NTS was applied. Most of these previous studies primarily aimed to identify unmonitored mid-polar AhR agonists. Consequently, by utilizing EDA combined with NTS, seven novel mid-polar AhR agonists were identified in sediments of Ulsan Bay, seven compounds in Lake Sihwa, and four compounds in Yeongil Bay (Cha et al., 2019; Kim et al., 2019; Gwak et al., 2022). The contribution of newly identified and targeted mid-polar AhR agonists to AhR-mediated potencies ranged from 3.5 to 32% in Ulsan Bay, 2.7 to 41% in Lake Sihwa, 0.1% in Masan Bay, 24 to 32% in Yeongil Bay, and 18 to 69% in Gamcheon Harbor (Busan Coast) (Fig. 5a). In all regions, t-PAHs in sediments exhibited a greater contribution to AhR-mediated potencies than e-PAHs and SOs.

To elucidate the distribution of the major AhR agonists present in the sediments of Gamcheon Harbor, Lake Sihwa, Masan Bay, Ulsan Bay, and

Table 1
Predicted potential toxic effects of four candidates of AhR agonists in sediments of Gamcheon Harbor using VEGA QSAR.

Predicted potential toxicity	VEGA QSAR models	Triphenylbenzene	Daphnoretin	Isorhamnetin	Trenebolone
Skin Sensitization	CAESAR	+[a]	+	+	+
	IRFMV-JRC	+	+	+	+
	NCSTOX	−[b]	+	+	+
Skin irritation	CONCERT/Kode	−	+	−	+
	CONCERT/coral	−	−	−	+
	CONCERT/SarPy	−	+	+	+
Eye irritation	CONCERT/Kode	−	+	−	−
	CONCERT/SarPy	−	+	−	−
Chromosomal aberration mode	Coral	−	+	+	+
Glucocorticoid receptor activity	Oberon	−	−	−	+
Endocrine disruptor activity screening	IRFMN	−	−	−	−
Hepatoxicity	IRFMN	n.a[c]	+	+	+
Androgen receptor activity	IRFMN/COMPARA	+	−	+	+
Carcinogenicity	IRFMN/Antares	−	+	+	−
	CAESAR	+	−	−	−
	ISS	−	+	+	−
	IRFMN/ISSCAN-CGX	+	+	+	+
Developmental toxicity	CAESAR	+	+	+	+
	PG	n.a	−	+	+
Estrogen receptor	IRFMN/CERAPP	n.a	−	+	−
	IRFMN	+	−	+	−
Mutagenicity	CAESAR	−	−	−	−
	CONSENSUS	+	−	−	−
	ISS	−	+	+	−
	KNN/Read-Across	+	−	+	−
	SarPy/IRFMN	−	−	−	−
Thyroid receptor activity	NRMEA	−	−	−	−

[a] +: active.
[b] −: non-active.
[c] n.a: not available.

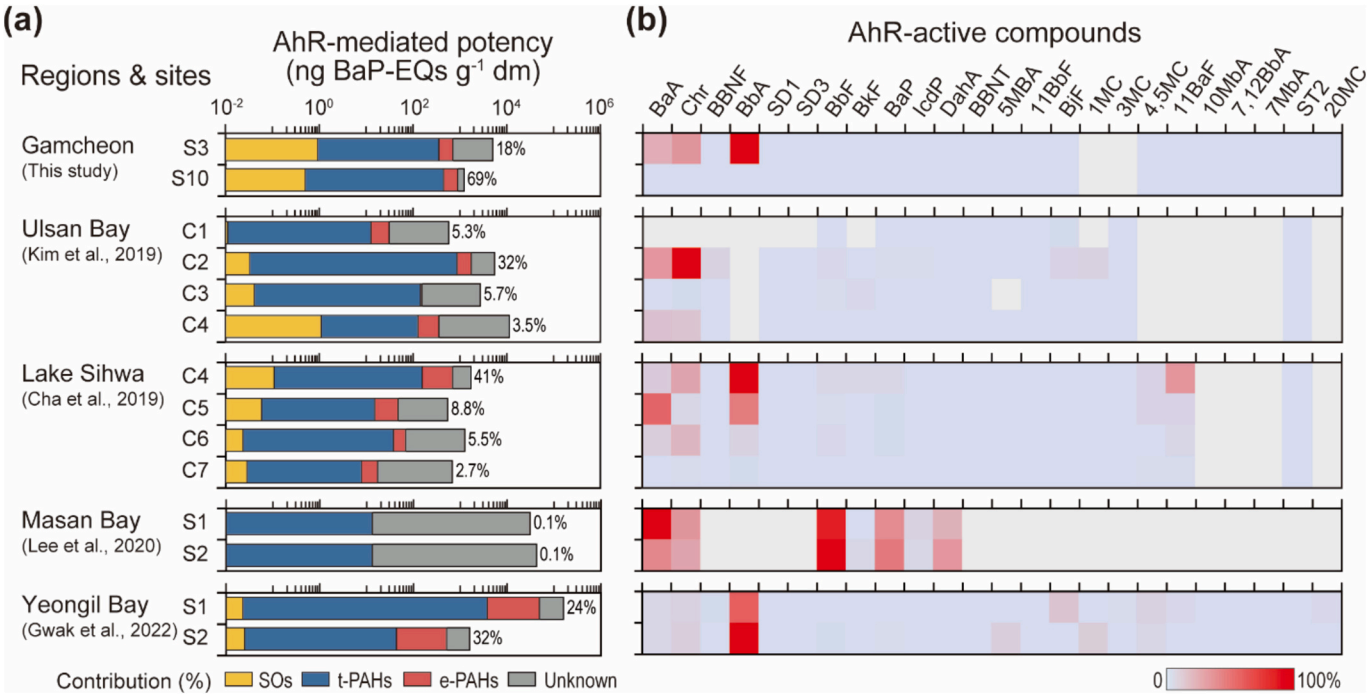

Fig. 5. (a) Comparison of AhR-mediated potencies and target AhR agonists (t-PAHs, e-PAHs, and SOs) contributions in sediments of Korean coastal waters [Ulsan Bay (Kim et al., 2019), Lake Sihwa (Cha et al., 2019), Masan Bay (Lee et al., 2020), and Yeongil Bay (Gwak et al., 2022)]. (b) Heatmap of the contribution of individual mid-polar AhR agonists in Korean coastal sediments.

Yeongil Bay, heat maps were used (Fig. 5b). Chrysene (Chr) was identified as the major AhR agonist in Ulsan Bay, benz[*b*]anthracene (BbA) in Lake Sihwa, Yeongil Bay, and Busan Coast, and benzo[*a*]anthracene (BaA) in Masan Bay. This region-specific variation is attributed to differences in the surrounding industrial activities. Notably, BbA originates from the film layer of OFET and OLED and is widely detected in many industrial complexes (Cha et al., 2019; Takahashi et al., 2007). Chr, largely sourced from vehicle and ship traffic and fuel combustion, alongside BaA, showed high concentrations of BaP-EQ_{chem} across most regions (Karacık et al., 2009). All these regions are located near harbors,

suggesting that these compounds flow into the harbor and accumulate in the coastal sediments. Previous studies have used EDA combined with NTS to identify AhR agonists in sediments from the Yellow Sea (e.g., 6-methylchrysene and 1,2-dimethylbenzo[*c*]phenanthrene) (Lee et al., 2022) and the Daqing River basin in China (e.g., 1-methyl-pyrene) (Xie et al., 2022). However, the identified AhR agonists only partially explained the observed AhR-mediated potencies, suggesting the presence of unknown AhR agonists.

The previous study aimed at identifying polar AhR agonists in F3 subfractions of Korean coastal sediments was conducted only in the sediments of Lake Sihwa (Table S15). Even though EDA combined with NTS was employed to identify novel AhR agonists in the F3 subfraction of Lake Sihwa sediments, the known target polar compounds were extremely limited, contributing only a small portion to AhR-mediated potencies (0.002–0.02%). Thus, this underscores the continued need for research to identify major polar AhR agonists in Korean coastal sediments using EDA.

4. Conclusions

Over the past few years, numerous studies have been conducted to identify previously unmonitored AhR agonists in Korean coastal sediments through the application of EDA. Nevertheless, AhR-mediated potencies in sediments still cannot be fully explained. The unexplained portion of AhR-mediated potencies might be attributed to the mixture effects of various compounds. AhR agonists are widely distributed in coastal sediments, indicating their association with diverse human activities. EDA could be employed in future hazardous substance monitoring programs, offering valuable insights for the management and regulation of unknown toxic substances.

CRediT authorship contribution statement

Jiyun Gwak: Writing – original draft, Visualization, Investigation, Formal analysis, Data curation, Conceptualization. **Junghyun Lee:** Writing – review & editing, Formal analysis, Data curation. **Jihyun Cha:** Investigation, Formal analysis, Data curation. **Hyo-Bang Moon:** Writing – review & editing, Investigation, Formal analysis, Data curation. **Jong Seong Khim:** Writing – review & editing, Project administration, Funding acquisition, Conceptualization. **Seongjin Hong:** Writing – review & editing, Writing – original draft, Supervision, Project administration, Funding acquisition, Conceptualization.

Declaration of competing interest

The authors declare that they have no known competing financial interests or personal relationships that could have appeared to influence the work reported in this paper.

Data availability

Data will be made available on request.

Acknowledgments

This study was supported by grants from the National Research Foundation of Korea (2021R1C1C1005977 and 2022R1A4A1033825) and the Korea Institute of Marine Science & Technology Promotion (KIMST) funded by the Ministry of Oceans and Fisheries (2021-0427, 2022-0534, RS-2023-00256330, and RS-2024-00417889).

Appendix A. Supplementary data

Supplementary data to this article can be found online at https://doi.org/10.1016/j.marpolbul.2024.117081.

References

Arturi, K., Hollender, J., 2023. Machine learning-based hazard-driven prioritization of features in nontarget screening of environmental high-resolution mass spectrometry data. Environ. Sci. Technol. 57, 18067–18079. https://doi.org/10.1021/acs.est.3c00304.

Booij, P., Vethaak, A.D., Leonards, P.E., Sjollema, S.B., Kool, J., de Voogt, P., Lamoree, M.H., 2014. Identification of photosynthesis inhibitors of pelagic marine algae using 96-well plate microfractionation for enhanced throughput in effect-directed analysis. Environ. Sci. Technol. 48, 8003–8011. https://doi.org/10.1021/es405428t.

CCME, 2001. Canadian sediment quality guidelines for the protection of aquatic life summary tables. Updated. In: Canadian Environmental Quality Guidelines, 1999. Canadian Council of Ministers of the Environment, Winnipeg. https://www.elaw.org/system/files/sediment_summary_table.pdf.

Cha, J., Hong, S., Kim, J., Lee, J., Yoon, S.J., Lee, S., Moon, H.B., Shin, K.H., Hur, J., Giesy, J.P., Khim, J.S., 2019. Major AhR-active chemicals in sediments of Lake Sihwa, South Korea: application of effect-directed analysis combined with full-scan screening analysis. Environ. Int. 133, 105199. https://doi.org/10.1016/j.envint.2019.105199.

Cha, J., Hong, S., Lee, J., Gwak, J., Kim, M., Kim, T., Hur, J., Giesy, J.P., Khim, J.S., 2021. Novel polar AhR-active chemicals detected in sediments of an industrial area using effect-directed analysis based on in vitro bioassays with full-scan high resolution mass spectrometric screening. Sci. Total Environ. 779, 146566. https://doi.org/10.1016/j.scitotenv.2021.146566.

Cha, J., Hong, S., Gwak, J., Kim, M., Lee, J., Kim, T., Han, G.M., Hong, S.H., Hur, J., Giesy, J.P., Khim, J.S., 2022. Identification of novel polar aryl hydrocarbon receptor agonists accumulated in liver of black-tailed gulls in Korea using advanced effect-directed analysis. J. Hazard. Mater. 429, 128305. https://doi.org/10.1016/j.jhazmat.2022.128305.

Cheng, F., Escher, B.I., Li, H., König, M., Tong, Y., Huang, J., He, L., Wu, X., Lou, X., Wang, D., Wu, F., Pei, Y., Yu, Z., Brooks, B.W., Zheng, E.Y., You, J., 2024. Deep learning bridged bioactivity, structure, and GC-HRMS-readable evidence to decipher nontarget toxicants in sediments. Environ. Sci. Technol. 58, 15415–15427. https://pubs.acs.org/doi/10.1021/acs.est.3c10814.

Choi, M., Moon, H.B., Yu, J., Eom, J.Y., Choi, H.G., 2010. Temporal trend of butyltins in seawater, sediments, and mussels from Busan Harbor of Korea between 2002 and 2007: tracking the effectiveness of tributyltin regulation. Arch. Environ. Contam. Toxicol. 58, 394–402. https://doi.org/10.1007/s00244-009-9428-2.

Eichbaum, K., Brinkmann, M., Buchinger, S., Reifferscheid, G., Hecker, M., Giesy, J.P., Engwall, M., van Bavel, B., Hollert, H., 2014. In vitro bioassays for detecting dioxin-like activity–application potentials and limits of detection, a review. Sci. Total Environ. 487, 37–48. https://doi.org/10.1016/j.scitotenv.2014.03.057.

Escher, B.I., Fenner, K., 2011. Recent advances in environmental risk assessment of transformation products. Environ. Sci. Technol. 45 (9), 3835–3847. https://doi.org/10.1021/es1030799.

Gago-Ferrero, P., Schymanski, E.L., Bletsou, A.A., Aalizadeh, R., Hollender, J., Thomaidis, N.S., 2015. Extended suspect and non-target strategies to characterize emerging polar organic contaminants in raw wastewater with LC-HRMS/MS. Environ. Sci. Technol. 49, 12333–12341. https://doi.org/10.1021/acs.est.5b03454.

Ghosh, P., Gupta, A., Thakur, I.S., 2015. Combined chemical and toxicological evaluation of leachate from municipal solid waste landfill sites of Delhi, India. Environ. Sci. Pollut. Res. 22 (12), 9148–9158. https://doi.org/10.1007/s11356-015-4077-7.

Gwak, J., Cha, J., Lee, J., Kim, Y., An, S.A., Lee, S., Moon, H.B., Hur, J., Giesy, J.P., Hong, S., Khim, J.S., 2022. Effect-directed identification of novel aryl hydrocarbon receptor-active aromatic compounds in coastal sediments collected from a highly industrialized area. Sci. Total Environ. 803, 149969. https://doi.org/10.1016/j.scitotenv.2021.149969.

Hashmi, M.A.K., Escher, B.I., Krauss, M., Teodorovic, I., Brack, W., 2018. Effect-directed analysis (EDA) of Danube River water sample receiving untreated municipal wastewater from Novi Sad, Serbia. Sci. Total Environ. 624, 1072–1081. https://doi.org/10.1016/j.scitotenv.2017.12.187.

Hashmi, M.A.K., Krauss, M., Escher, B.I., Teodorovic, I., Brack, W., 2020. Effect-directed analysis of progestogens and glucocorticoids at trace concentrations in river water. Environ. Toxicol. Chem. 39 (1), 189–199. https://doi.org/10.1002/etc.4609.

Heberer, T., 2002. Occurrence, fate, and removal of pharmaceutical residues in the aquatic environment: a review of recent research data. Toxicol. Lett. 131, 5–17. https://doi.org/10.1016/S0378-4274(02)00041-3.

Hong, S.H., Yim, U.H., Shim, W.J., Oh, J.R., 2005. Congener-specific survey for polychlorinated biphenyls in sediments of industrialized bays in Korea: regional characteristics and pollution sources. Environ. Sci. Technol. 39, 7380–7388. https://doi.org/10.1021/es050397c.

Hong, S., Khim, J.S., Ryu, J., Park, J., Song, S.J., Kwon, B.O., Choi, K., Ji, K., Seo, J., Lee, S., 2012. Two years after the Hebei Spirit oil spill: residual crude-derived hydrocarbons and potential AhR-mediated activities in coastal sediments. Environ. Sci. Technol. 46, 1406–1414. https://doi.org/10.1021/es203491b.

Hong, S., Lee, J., Lee, C., Yoon, S.J., Jeon, S., Kwon, B.O., Lee, J.H., Giesy, J.P., Khim, J.S., 2016a. Are styrene oligomers in coastal sediments of an industrial area aryl hydrocarbon-recep-tor agonists? Environ. Pollut. 213, 913–921. https://doi.org/10.1016/j.envpol.2016.03.025.

Hong, S., Giesy, J.P., Lee, J.S., Lee, J.H., Khim, J.S., 2016b. Effect-directed analysis: current status and future challenges. Ocean Sci. J. 51, 413–433. https://doi.org/10.1007/s12601-016-0038-4.

Hong, S., Lee, Y., Yoon, S.J., Lee, J., Kang, S., Won, E.J., Hur, J., Khim, J.S., Shin, K.H., 2019. Carbon and nitrogen stable isotope signatures linked to anthropogenic toxic

substances pollution in a highly industrialized area of South Korea. Mar. Pollut. Bull. 144, 152–159. https://doi.org/10.1016/j.marpolbul.2019.05.006.
Hong, S., Lee, J., Cha, J., Gwak, J., Khim, J.S., 2023. Effect-directed analysis combined with nontarget screening to identify unmonitored toxic substances in the environment. Environ. Sci. Technol. 57, 19148–19155. https://doi.org/10.1021/acs.est.3c05035.
Ibáñez, M., Sancho, J.V., Hernández, F., McMillan, D., Rao, R., 2008. Rapid non-target screening of organic pollutants in water by ultraperformance liquid chromatography coupled to time-of-flight mass spectrometry. Trac-Trend. Anal. Chem. 27, 481–489. https://doi.org/10.1016/j.trac.2008.03.007.
Jeon, S., Hong, S., Kwon, B.O., Park, J., Song, S.J., Giesy, J.P., Khim, J.S., 2017. Assessment of potential biological activities and distributions of endocrine-disrupting chemicals in sediments of the west coast of South Korea. Chemosphere 168, 441–449. https://doi.org/10.1016/j.chemosphere.2016.10.089.
Kado, N.Y., Okamoto, R.A., Karim, J., Kuzmicky, P.A., 2000. Airborne particle emissions from 2-and 4-stroke outboard marine engines: polycyclic aromatic hydrocarbon and bioassay analyses. Environ. Sci. Technol. 34 (13), 2714–2720. https://doi.org/10.1021/es9909834.
Karacık, B., Okay, O.S., Henkelmann, B., Bernhöft, S., Schramm, K.W., 2009. Polycyclic aromatic hydrocarbons and effects on marine organisms in the Istanbul Strait. Environ. Int. 35, 599–606. https://doi.org/10.1016/j.envint.2008.11.005.
Kim, J., Hong, S., Cha, J., Lee, J., Kim, T., Lee, S., Moon, H.B., Shin, K.H., Hur, J., Lee, J. S., Giesy, J.P., Khim, J.S., 2019. Newly identified AhR-active compounds in the sediments of an industrial area using effect-directed analysis. Environ. Sci. Technol. 53, 10043–10052. https://doi.org/10.1021/acs.est.9b02166.
Kim, M., Jee, S.C., Kim, K.S., Kim, H.S., Yu, K.N., Sung, J.S., 2021. Quercetin and isorhamnetin attenuate benzo[a]pyrene-induced toxicity by modulating detoxification enzymes through the AhR and NRF2 signaling pathways. Antioxidants 10 (5), 787. https://doi.org/10.3390/antiox10050787.
Klanovicz, N., Pinto, C.A., 2024. Occurrence of pharmaceutically active compounds in groundwater and their effects to the human health. Environ. Sci. Pollut. Res. 31, 1–16. https://doi.org/10.1007/s11356-024-33423-6.
Kwon, B.G., Koizumi, K., Chung, S.Y., Kodera, Y., Kim, J.O., Saido, K., 2015. Global styrene oligomers monitoring as new chemical contamination from polystyrene plastic marine pollution. J. Hazard. Mater. 300, 359–367. https://doi.org/10.1016/j.jhazmat.2015.07.039.
Larsen, R.K., Baker, J.E., 2003. Source apportionment of polycyclic aromatic hydrocarbons in the urban atmosphere: a comparison of three methods. Environ. Sci. Technol. 37, 1873–1881. https://doi.org/10.1021/es0206184.
Ledesma, E.B., Kalish, M.A., Nelson, P.F., Wornat, M.J., Mackie, J.C., 2000. Formation and fate of PAH during the pyrolysis and fuel-rich combustion of coal primary tar. Fuel 79, 1801–1814. https://doi.org/10.1016/S0016-2361(00)00044-2.
Lee, J., Khim, J.S., 2022. Revisited a sediment quality triad approach in the Korean coastal waters: past research, current status, and future directions. Environ. Pollut. 292, 118262. https://doi.org/10.1016/j.envpol.2021.118262.
Lee, J., Hong, S., Kim, T., Lee, C., An, S.A., Kwon, B.O., Lee, S., Moon, H.B., Giesy, J.P., Khim, J.S., 2020. Multiple bioassays and targeted and nontargeted analyses to characterize potential toxicological effects associated with sediments of Masan Bay: focusing on AhR-mediated potency. Environ. Sci. Technol. 54, 4443–4454. https://doi.org/10.1021/acs.est.9b07390.
Lee, J., Hong, S., Kim, T., Park, S.Y., Cha, J., Kim, Y., Gwak, J., Lee, S., Moon, H.B., Hu, W., Wang, T., Giesy, J.P., Khim, J.S., 2022. Identification of AhR agonists in sediments of the Bohai and Yellow Seas using advanced effect-directed analysis and in silico prediction. J. Hazard. Mater. 435, 128908. https://doi.org/10.1016/j.jhazmat.2022.128908.
Li, J., Dong, H., Xu, X., Han, B., Li, X., Zhu, C., Han, C., Liu, S., Yang, D., Xu, Q., Zhang, D., 2016. Prediction of the bioaccumulation of PAHs in surface sediments of Bohai Sea, China and quantitative assessment of the related toxicity and health risk to humans. Mar. Pollut. Bull. 104, 92–100. https://doi.org/10.1016/j.marpolbul.2016.02.005.
Marzo, M., Kulkarni, S., Manganaro, A., Roncaglioni, A., Wu, S., Barton-Maclaren, T.S., Lester, C., Benfenati, E., 2016. Integrating in silico models to enhance predictivity for developmental toxicity. Toxicology 370, 127–137. https://doi.org/10.1016/j.tox.2016.09.015.
Mekenyan, O.G., Veith, G.D., Call, D.J., Ankley, G.T., 1996. A Qsar evaluation of Ah receptor binding of halogenated aromatic xenobiotics. Environ. Health Persp. 104, 1302–1310. https://doi.org/10.1289/ehp.961041302.
Mimura, J., Fujii-Kariyama, Y., 2003. Functional role of AhR in the expression of toxic effects by TCDD. Biochim. Biophys. Acta 1619, 263–268. https://doi.org/10.1016/S0304-4165(02)00485-3.
Moon, H.B., Kannan, K., Choi, M., Choi, H.G., 2007. Polybrominated diphenyl ethers (PBDEs) in marine sediments from industrialized bays of Korea. Mar. Pollut. Bull. 54 (9), 1402–1412. https://doi.org/10.1016/j.marpolbul.2007.05.024.
Moschet, C., Lew, B.M., Hasenbein, S., Anumol, T., Young, T.M., 2017. LC- and GC-QTOF-MS as complementary tools for a comprehensive micropollutant analysis in aquatic systems. Environ. Sci. Technol. 51, 1553–1561. https://doi.org/10.1021/acs.est.6b05352.
Muz, M., Krauss, M., Kutsarova, S., Schulze, T., Brack, W., 2017. Mutagenicity in surface waters: synergistic effects of carboline alkaloids and aromatic amines. Environ. Sci. Technol. 51 (3), 1830–1839. https://doi.org/10.1021/acs.est.6b05468.
Pizzo, F., Lombardo, A., Manganaro, A., Benfenati, E., 2013. In silico models for predicting ready biodegradability under REACH: a comparative study. Sci. Total Environ. 463–464, 161–168. https://doi.org/10.1016/j.scitotenv.2013.05.060.
Samanipour, S., O'Brien, J.W., Reid, M.J., Thomas, K.V., Praetorius, A., 2022. From molecular descriptors to intrinsic fish toxicity of chemicals: an alternative approach to chemical prioritization. Environ. Sci. Technol. 57, 17950–17958. https://doi.org/10.1021/acs.est.2c07353.
Schymanski, E.L., Singer, H.P., Slobodnik, J., Ipolyi, I.M., Oswald, P., Krauss, M., Schulze, T., Haglund, P., Letzel, T., Grosse, S., Thomaidis, N.S., Bletsou, A., Zwiener, C., Ibáñez, M., Portolés, T., de Boer, R., Reid, M.J., Onghena, M., Kunkel, U., Schulz, W., Guillon, A., Noyon, N., Leroy, G., Bados, P., Bogialli, S., Stipanicev, D., Rostkowski, P., Hollender, J., 2015. Non-target screening with high-resolution mass spectrometry: critical review using a collaborative trial on water analysis. Anal. Bioanal. Chem. 407, 6237–6255. https://doi.org/10.1007/s00216-015-8681-7.
Solberg, T., Tiefenthaler Jr., J., O'Brien, G., Behnke, H., Poulson, H., Ela, J., Willett, S., 2003. Consensus-based Sediment Quality Guidelines. Recommendations for Use & Application Interim Guidance. Developed by the Contaminated Sediment Standing Team. Wisconsin Department of Natural Resources. https://dnr.wi.gov/files/PDF/pubs/rr/RR088.pdf.
Takahashi, T., Takenobu, T., Takeya, J., Iwasa, Y., 2007. Ambipolar light-emitting transistors of a tetracene single crystal. Adv. Funct. Mater. 17 (10), 1623–1628. https://doi.org/10.1002/adfm.200700046.
Vedani, A., Dobler, M., Hu, Z., Smieško, M., 2015. OpenVirtualToxLab-a platform for generating and exchanging in silico toxicity data. Toxicol. Lett. 232, 519–532. https://doi.org/10.1016/j.toxlet.2014.09.004.
Von Oepen, B., Kördel, W., Klein, W., 1991. Sorption of nonpolar and polar compounds to soils: processes, measurements and experience with the applicability of the modified OECD-Guideline 106. Chemosphere 22, 285–304. https://doi.org/10.1016/0045-6535(91)90318-8.
Weiss, J.M., Hamers, T., Thomas, K.V., Van der Linden, S., Leonards, P.E., Lamoree, M. H., 2009. Masking effect of anti-androgens on androgenic activity in European river sediment unveiled by effect-directed analysis. Anal. Bioanal. Chem. 394, 1385–1397. https://doi.org/10.1007/s00216-009-2807-8.
Wolf, S., Schmidt, S., Müller-Hannemann, M., Neumann, S., 2010. In silico fragmentation for computer assisted identification of metabolite mass spectra. BMC Bioinformatics 11, 148. https://doi.org/10.1186/1471-2105-11-148.
Xiao, H., Brinkmann, M., Thalmann, B., Schiwy, A., GrosseBrinkhaus, S., Achten, C., Eichbaum, K., Gembe, C., Seiler, T.B., Hollert, H., 2017. Toward streamlined identification of dioxin-like compounds in environmental samples through integration of suspension bioassay. Environ. Sci. Technol. 51 (6), 3382–3390. https://doi.org/10.1021/acs.est.6b06003.
Xie, R., Xu, Y., Ma, M., Wang, Z., 2022. An integrated screening strategy for novel AhR agonist candidate identification and toxicity confirmation in sediments. Sci. Total Environ. 842, 156816. https://doi.org/10.1016/j.scitotenv.2022.156816.
Yu, S., Hong, B., Ma, J., Chen, Y., Xi, X., Gao, J., Xiuqin, H., Xiangrong, X., Sun, Y., 2017. Surface sediment quality relative to port activities: a contaminant-spectrum assessment. Sci. Total Environ. 596, 342–350. https://doi.org/10.1016/j.scitotenv.2017.04.076.
Zhao, Z., Gong, X., Zhang, L., Jin, M., Cai, Y., Wang, X., 2021. Riverine transport and water-sediment exchange of polycyclic aromatic hydrocarbons (PAHs) along the middle-lower Yangtze River, China. J. Hazard. Mater. 403, 123973. https://doi.org/10.1016/j.jhazmat.2020.123973.
Zwart, N., Jonker, W., Broek, R.T., de Boer, J., Somsen, G., Kool, J., Hamers, T., Houtman, C.J., Lamoree, M.H., 2020. Identification of mutagenic and endocrine disrupting compounds in surface water and wastewater treatment plant effluents using high-resolution effect-directed analysis. Water Res. 168, 115204. https://doi.org/10.1016/j.watres.2019.115204.

<Supplementary Materials>

Effect-directed analysis and nontarget screening for identifying AhR-active substances in sediments of Gamcheon Harbor, South Korea

Jiyun Gwak, Junghyun Lee, Jihyun Cha, Hyo-Bang Moon, Jong Seong Khim*, Seongjin Hong*

This PDF file includes:

Number of pages: 18

Number of Supplementary Tables: 15, Table S1 to S15

Number of Supplementary Figure: 1, Fig. S1

References

*** Corresponding Authors.**

E-mail addresses: hongseongjin@cnu.ac.kr (S. Hong); jskocean@snu.ac.kr (J.S. Khim).

Supplementary Tables

Table S1. Reverse phase(RP)-HPLC conditions for fractionation of silica gel column fractions (Hong et al., 2016).

Instrument	Agilent 1260 HPLC system (Preparative scale) 1260 Multiple wavelength detector
Column	PrepHT XDB-C18 reverse phase column (250 mm × 21.2 mm × 7 μm)
Mobile phase	A: Water, B: Methanol
Flow rate	10 mL min^{-1}
Injection volume	1 mL
Mobile phase gradient	40% A (0 min) → 40–0% A (0–40 min) → 0% A (40–60 min) → 0–40% A (60–62 min) → 40% A (62–70 min) 60% B (0 min) → 60–100% B (0–40 min) → 100% B (40–60 min) → 100–60% B (60–62 min) → 60% B (62–70 min)
Test standards	34 polychlorinated biphenyls 16 polycyclic aromatic hydrocarbons 7 alkylphenols 5 phthalates
Fractions collected times	

Sub-fraction	Sampling time (min.)	Volume (mL)	Log K_{OW}
1	3.11 – 6.35	38	<1
2	6.35 – 12.83	65	1 – 2
3	12.83 – 19.32	65	2 – 3
4	19.32 – 25.80	65	3 – 4
5	25.80 – 32.29	65	4 – 5
6	32.29 – 38.78	65	5 – 6
7	38.78 – 45.26	65	6 – 7
8	45.26 – 51.70	65	7 – 8
9	51.70 – 58.23	65	8 – 9
10	58.23 – 64.72	65	>9

Table S2. Experimental design for H4IIE-*luc in vitro* bioassay.

Bioassay		**In vitro assays (H4IIE-*luc*)**
Culture condition	**Temperature**	37 °C
	Gas carrier	5% CO_2
	Culture flask	TC-treated culture dish
Seeding condition	**Test chamber**	96-well plate
	Initial concentrations	7.0×10^4 cells mL^{-1}
	Volume	250 μL $well^{-1}$
	Incubation time	24 h
Dosing	**Positive control**	Benzo[*a*]pyrene (50, 17, 6.0, 2.0, 0.62, and 0.21 nM)
	Samples	Raw extracts, silica gel fractions, and RP-HPLC fractions
	Solvent control	0.1% DMSO
	Volume	250 μL $well^{-1}$
	Replicates	3
	Test duration	4 h
Measurement	**Endpoint**	Luciferase activity
	Instrument	VictorX3 multilabel plate reader (PerkinElmer, Waltham, MA)

Table S3. Target compounds, abbreviations, target ions, and method detection limits in the GC-MSD analysis.

Target compounds	Abbreviation	Target ions		Method detection limit ($ng\ g^{-1}$ dm)
		Quantification ion	Confirmation ion	
Traditional PAHs (t-PAHs)				
Acenaphthene	Ace	153	154, 152	0.60
Acenaphthylene	Acl	152	151, 150	0.76
Fluorene	Flu	166	165, 167	0.65
Phenanthrene	Phe	178	176, 179	0.63
Anthracene	Ant	178	176, 179	0.70
Fluoranthene	Fl	202	200, 101	0.42
Pyrene	Py	202	200, 101	0.39
Benzo[*a*]anthracene	BaA	228	226, 229	0.27
Chrysene	Chr	228	226, 229	0.22
Benzo[*b*]fluoranthene	BbF	252	253, 250	0.19
Benzo[*k*]fluoranthene	BkF	252	253, 251	0.19
Benzo[*a*]pyrene	BaP	252	253, 126	0.17
Indeno[*1,2,3-cd*]pyrene	IcdP	276	138, 137	0.20
Dibenz[*a,h*]anthracene	DbahA	278	276, 279	0.33
Benzo[*g,h,i*]perylene	BghiP	276	138, 137	0.10
Emerging PAHs (e-PAHs)				
2-Methylanthracene	2MA	192	191, 189	2.2
9-Ethylphenanthrene	9EP	191	206, 189	0.9
Benzo[*b*]naphtho[*2,3-d*]furan	BBNF	218	189, 219	0.34
11H-Benzo[*b*]fluorene	11BbF	216	215, 213	0.28
Benzo[*b*]naphtho[*2,1*-d]thiophene	BBNT	234	235, 232	0.17
5-Methylbenz[*a*]anthracene	5MBA	256	241, 239	0.11
1,12-dimethylbenzo[*c*]phenanthrene	BCP	242	241, 239	0.11
Benzo[*j*]fluoranthene	BjF	252	253, 250	2.1
Benzo[*e*]pyrene	BEP	252	250, 253	3.7
11H-benzo[*a*]fluorene	11BaF	216	215, 216	0.15
1-Methylpyrene	1MP	216	215,189	0.12
Cyclopenta[*cd*]pyrene	CcdP	226	259	0.10
4,5-Methanochrysene	4,5MC	239	240, 241	0.10
Benz[*b*]anthracene	BbA	228	226, 229	0.32
7,12-dimethylbenz[*a*]anthracene	7,12DbA	256	241, 239	0.12
10-methylbenz[*a*]pyrene	10MbA	266	265, 263	0.12
7-methylbenz[*a*]anthracene	7MbA	242	241, 239	0.17
20-methylcholanthrene	20MC	268	252, 253	0.30
Styrene oligomers (SOs)				
1,3-Diphenylpropane	SD1	92	196, 105	0.19
cis-1,2-Diphenylcyclobutane	SD2	104	208, 78	0.18
2,4-Diphenyl-1-butene	SD3	91	208, 104	0.89
trans-1,2-Diphenylcyclobutane	SD4	104	208, 78	0.11
2,4,6-Triphenyl-1-hexene	ST1	91	117, 194	0.63
1e-Phenyl-4e-(1-phenylethyl)-tetralin	ST2	91	129, 207	0.66
1a-Phenyl-4e-(1-phenylethyl)-tetralin	ST3	91	129, 207	0.31
1a-Phenyl-4a-(1-phenylethyl)-tetralin	ST4	91	129, 207	0.70
1e-Phenyl-4a-(1-phenylethyl)-tetralin	ST5	91	129, 207	0.41
1,3,5-Triphenylcyclohexane	ST6	117	104, 130	0.88

Table S4. Instrumental conditions of GC-MSD for analysis of PAHs and SOs.

Instrument	GC: Agilent Technologies 7890B MSD: Agilent Technologies 5977A
Column	DB-5MS (30 m × 0.25 mm i.d. × 0.25 μm film)
Carrier gas	He
Flow rate	1.0 mL $min.^{-1}$
Injection volume	1 μL
Mass range	50−600 *m*/*z*
Ion source temperature	230 °C
Ionization mode	EI mode (70 eV)
Oven temperature	60 ℃ (hold 2 min) → 6 °C min^{-1} to 300 °C (hold 13 min)

Table S5. Instrumental conditions of HPLC-MS/MS for quantification of polar AhR agonists in sediment.

Compounds	MRM		Method detection limit ($ng\ g^{-1}$)
	Transition Parent ion	Daughter ion (ESI+)	
Polar AhR agonists			
Ciprofloxacin	332.00	314.00	0.062
Genistein	270.92	153.00	0.029
Mepanipyrim	223.95	106.00	0.007
Protopine	353.95	189.10	0.060
Rutaecarpine	287.98	272.90	0.025
Internal standard			
Monolinuron	215.00	126.20	

Table S6. Instrumental conditions for analyzing polar AhR agonists using HPLC-MS/MS (Cha et al., 2021).

Instrument	HPLC: Agilent Infinity 1290 II, MS/MS: SCIEX Qtrap 6500
Samples	F3.6 and F3.7 RP-HPLC fractions of S3 and S10
Column	ZORBAX Eclipse XDB-C18 (150 mm × 2.1 mm i.d. × 5 μm film)
Column temperature	40 ℃
Injection volume	3 μL
Flow rate	0.4 mL min^{-1}
Mobile phase	A: 0.1% Formic acid and 10 mM ammonium formate in water B: 0.1% Formic acid in acetonitrile
Mobile phase gradient	Time (min) / Solvent A / Solvent B 0 / 90 / 10 1 / 90 / 10 15 / 0 / 100 24 / 0 / 100 25 / 90 / 10 30 / 90 / 10
Ionization mode	Electrospray ionization (ESI) Positive mode
Ion source gas	50 psi
Curtain gas	30 psi
Temperature	500 °C
Ion source	DuoSpray Ion Source
Ion spray voltage	Positive: 5,500 V

Table S7. Instrumental conditions of GC-QTOFMS for nontarget screening.

Instrument	GC: Agilent Technologies 7890B QTOFMS: Agilent Technologies 7200
Samples	S3 (F2.7 and F2.8)
Column	DB-5MS UI (30 m × 0.25 mm i.d. × 0.25 μm film)
Carrier gas	He
Flow rate	1.2 mL $min.^{-1}$
Injection volume	2 μL
Mass range	50–800 *m/z*
Ion source temperature	230 °C
Ionization mode	EI mode (70 eV)
Software	Qualitative analysis B.07.01 MassHunter Quantitative analysis Unknown analysis NIST Library (ver. 2014)

Table S8. Instrumental conditions of LC-QTOFMS for nontarget screening.

Instrument	LC: 1290 infinity II (Agilent Technologies, Santa Clara, CA) QTOFMS: Triple time-of-flight (TripleTOF®) 5600+ mass spectrometer (AB Sciex, Framingham, MA)
Samples	S3 (F3.6 and F3.7)
Analytical column	ZORBAX Eclipse XDB-C18 (150 mm × 2.1 mm i.d. × 5 μm film)
Column temperature	40 °C
Injection volume	3 μL
Flow rate	0.4 mL min^{-1}
Mobile phase	A: 0.1% Formic acid and 10 mM ammonium formate in water, B: 0.1% Formic acid in acetonitrile
Mobile phase gradient	Time (min) / Solvent A / Solvent B 0 / 90 / 10 1 / 90 / 10 15 / 0 / 100 24 / 0 / 100 25 / 90 / 10 30 / 90 / 10
Ionization mode	Electrospray ionization (ESI) Positive and Negative mode
Mass scan type	Full scan and Information Dependent Acquisition (IDA) Scanning
TOF masses (Da)	100-2000 Da
Ion source gas 1	50 psi
Ion source gas 2	50 psi
Curtain gas	30 psi
Temperature	500 °C
Ion source	DuoSpray Ion Source
Ion spray voltage	Positive: 5,500 V, Negative -4,500 V
Software	All-in-One_HRMS/MS TCM library 1.0 metabolite software

Table S9. Molecular formula, molecular mass, and relative potency values for mid-polar AhR agonists reported previously (compared to benzo[a]pyrene).

Compounds	Molecular formula	Molecular mass	ReP values	References
Traditional PAHs				
Benz[*a*]anthracene	$C_{18}H_{12}$	228	3.2×10^{-1}	Kim et al. (2019)
Chrysene	$C_{18}H_{12}$	228	8.5×10^{-1}	
Benzo[*b*]fluoranthene	$C_{20}H_{12}$	252	5.0×10^{-1}	
Benzo[*k*]fluoranthene	$C_{20}H_{12}$	252	4.8×10^{-1}	
Benzo[*a*]pyrene	$C_{20}H_{12}$	252	1.0	
Indeno[*1,2,3-c,d*]pyrene	$C_{22}H_{12}$	276	5.8×10^{-1}	
Dibenz[*a,h*]anthracene	$C_{22}H_{14}$	278	6.6×10^{-1}	
Emerging PAHs				
Benzo[*b*]naphtho[*2,3-d*]furan	$C_{16}H_{10}O$	218	8.2×10^{-2}	Kim et al. (2019)
11H-Benzo[*b*]fluorene	$C_{17}H_{12}$	216	2.4×10^{-1}	
Benzo[*b*]naphtho[*2,1-d*]thiophene	$C_{16}H_{10}S$	234	3.6×10^{-2}	
3-Methylchrysene	$C_{19}H_{14}$	242	1.5	
5-Methylbenz[*a*]anthracene	$C_{19}H_{14}$	242	4.2×10^{-1}	
1-Methylchrysene	$C_{19}H_{14}$	242	6.0	
Benzo[*j*]fluoranthene	$C_{20}H_{12}$	252	1.7	
11H-Benzo[*a*]fluorene	$C_{17}H_{12}$	216	1.2	Cha et al. (2019)
Benz[*b*]anthracene	$C_{18}H_{12}$	228	10.6	
4,5-Methanochrysene	$C_{19}H_{12}$	234	1.0	Gwak et al. (2022)
7,12-Dimethylbenz[*a*]anthracene	$C_{20}H_{16}$	256	3.2	
7-Methylbenz[*a*]anthracene	$C_{19}H_{14}$	242	1.4	
10-Methylbenzo[*a*]pyrene	$C_{18}H_{12}$	266	12	
20-Methylcholanthrene	$C_{21}H_{16}$	268	0.2	
Styrene Oligomers				
1,3-Diphenylpropane	$C_{15}H_{16}$	196	2.3×10^{-3}	Hong et al. (2016)
2,4-Diphenyl-1-butene	$C_{16}H_{16}$	208	3.0×10^{-4}	
1e-Phenyl-4e-(1-phenylethyl)-tetralin	$C_{24}H_{24}$	312	2.7×10^{-3}	

Table S10. Molecular formula, molecular mass, and relative potency values for polar AhR agonists reported previously (compared to benzo[a]pyrene).

Compounds	Molecular formula	Molecular mass	ReP values	Reference
Polar e-PAHs				
Ciprofloxacin	$C_{17}H_{18}FN_3O_3$	331.341	5.0×10^{-3}	Cha et al. (2021)
Genistein	$C_{15}H_{10}O_5$	270.237	1.0×10^{-4}	
Mepanipyrim	$C_{14}H_{13}N_3$	223.273	4.0×10^{-4}	
Protopine	$C_{20}H_{19}NO_5$	353.369	2.0×10^{-5}	
Rutaecarpine	$C_{18}H_{13}N_3O$	287.315	1.9	

Table S11. Concentrations of persistent toxic substances (PTSs) in sediments of Gamcheon Harbor, Korea (ng g^{-1} dm).

Compounds		Sites											
		S1	**S2**	**S3**	**S4**	**S5**	**S6**	**S7**	**S8**	**S9**	**S10**	**S11**	**S12**
t-PAHs	Acl	3.2	3.87	4.6	1.34	0.26	5.5	2.4	3.6	6.6	4.2	2.1	0.76
	Ace	12	8.3	23	1.9	1	10	0.75	8.8	11	16	3.4	0.73
	Flu	13	12	15	6.1	0.97	17	0.42	10	14	11	6.5	3
	Phe	75	73	130	36	7.5	110	46	68	80	79	41	12
	Ant	18	18	31	6.8	2.1	26	3.3	15	32	18	10	2.5
	Fl	130	150	260	47	14	180	0.25	130	140	170	77	19
	Py	150	170	260	61	14	180	0.61	140	150	150	80	20
	BaA[a]	60	79	130	20	6.2	79	0.55	60	86	89	38	11
	Chr[a]	35	40	63	12	3.3	38	0.2	37	55	52	22	7.3
	BbF[a]	130	110	190	39	12	100	0.82	140	150	160	73	23
	BkF[a]	36	34	49	12	3.6	32	0.97	37	48	46	20	6.4
	BaP[a]	67	81	140	21	6.5	80	3.3	66	110	98	40	9
	IcdP[a]	110	100	190	36	11	106	19	120	150	160	68	23
	DbahA[a]	20	19	34	6.5	1.8	18	33	21	28	29	11	3.3
	BghiP	89	82	140	30	7.9	83	14	89	110	110	51	17
e-PAHs	2MA	5.6	6.2	6.1	2.3	0.43	5.9	2.7	3.8	9.6	4.1	3.8	0.65
	9EP	13	13	7.7	5.4	0.67	8.7	0.12	9.4	1	6.6	7.7	2.2
	BBNF[a]	8.6	9.5	13	2.9	0.75	9.8	<LOD[b]	8.3	11	9.3	4.9	1.5
	11BbF[a]	13	18	27	5	1.5	20	0.85	13	24	20	8.2	1.9
	BBNT[a]	13	14	19	3.9	1.1	9.7	0.75	7.8	15	15	6.1	1.3
	5MBA[a]	3.9	4.6	3.8	1.3	0.24	3	0.22	2.7	4.7	2.8	2.1	0.47
	BCP	1.1	1.3	2.1	0.4	0.12	1.2	0.23	1.2	1.8	1.7	0.74	0.13
	BjF[a]	43	42	70	14	3.9	44	<LOD	47	66	56	29	8.3
	BEP	87	80	130	27	7.7	76	<LOD	91	110	110	49	14
	1MP	8.3	9.7	7.4	3.3	5.1	7.3	0.63	5.9	8.5	4.6	5	1.3
	CcdP	17	42	62	12	17	39	4.2	17	49	23	22	4.5
	11BaF[a]	24	17	20	8.4	10	16	1.3	12	20	25	15	4.1
	4,5MC[a]	15	18	24	7.4	14	17	3.6	16	23	13	10	3.8
	BbA[a]	12	12	16	9.2	12	12	8.6	11	12	13	10	8.5
	7MbA[a]	13	12	12	11	11	11	11	11	11	12	11	10
	7,12DbA[a]	23	17	17	16	17	18	15	17	17	15	16	15
	20MC[a]	18	22	22	17	20	23	16	26	22	15	18	15
	10MbA[a]	27	57	42	18	22	24	14	26	66	15	14	15
SOs	SD1[a]	1.2	0.95	0.81	1.1	1.9	0.85	3.3	1.4	0.72	0.69	0.52	0.28
	SD2	0.75	0.79	0.5	0.75	1.3	0.96	0.03	1.2	1.13	0.67	0.4	0.19
	SD3[a]	120	97	76	19	360	190	3.4	160	260	160	120	30
	SD4	1.8	2.1	1.7	2.6	2.6	2.2	0.07	3.1	1.7	1.1	1.1	0.67
	ST1	7.8	3.5	5.1	2.2	16	2.3	3.4	4.1	3.4	3.4	2.5	1.3
	ST2[a]	54	11	66	14	54	13	5.1	92	20	99	45	1.2
	ST3	27	1.6	30	6.4	25	10	0.63	40	15	42	19	0.35
	ST4	28	10	31	6.3	27	12	0.73	43	31	48	21	1.3
	ST5	270	28	40	8.5	33	15	0.65	48	24	48	24	1.6

[a] AhR-active compounds.
[b] <LOD: Below detection limits.

Table S12. Concentrations of target polar AhR agonists in sediments of Gamcheon Harbor, Korea (ng g^{-1} dm).

Compounds	Sites											
	S1	**S2**	**S3**	**S4**	**S5**	**S6**	**S7**	**S8**	**S9**	**S10**	**S11**	**S12**
Ciprofloxacin	<LOD	0.07	<LOD	<LOD	<LOD	<LOD	<LOD	<LOD	<LOD	<LOD[a]	<LOD	<LOD
Genistein	<LOD	<LOD	<LOD	<LOD	<LOD	<LOD	<LOD	<LOD	<LOD	<LOD	<LOD	<LOD
Mepanipyrim	<LOD	0.01	<LOD	<LOD	<LOD	<LOD	<LOD	<LOD	<LOD	<LOD	<LOD	<LOD
Protopine	<LOD	<LOD	<LOD	<LOD	<LOD	<LOD	<LOD	<LOD	<LOD	<LOD	<LOD	<LOD
Rutaecarpine	0.04	0.2	0.03	<LOD	0.2	<LOD	<LOD	<LOD	0.02	<LOD	<LOD	<LOD

[a] <LOD: Below detection limit

Table S13. Potency balance between instrument-derived BaP-EQs and bioassay-derived BaP-EQs in the RP-HPLC fractions (F2.6−F2.8 and of S3 and S10 and F3.6−F3.7 of S3) of the sediments in Gamcheon Harbor, Korea.

Compounds	Abb[a]	S3			S10			S3	
		F2.6	F2.7	F2.8	F2.6	F2.7	F2.8	F3.6	F3.7
Instrument-derived BaP-EQs (ng BaP-EQ g^{-1} dm)									
Traditional PAHs and SOs									
Benz[*a*]anthracene	BaA	45			31				
Chrysene	Chr	59			49				
1,3-Diphenylpropane	SD1	0.004			0.003				
2,4-Diphenyl-1-butene	SD3	0.36			0.74				
Benzo[*b*]fluoranthene	BbF		94						
Benzo[*k*]fluoranthene	BkF		24						
Benzo[*a*]pyrene	BaP		140						
Indeno[*1,2,3-c,d*]pyrene	IcdP		99						
Dibenz[*a,h*]anthracene	DahA		20						
2,4,6-Triphenyl-1-hexene	ST2								
Emerging PAHs									
Benzo[*b*]naphtho[*2,3-d*]furan	BBNF	1.2			0.88				
Benz[*b*]anthracene	BbA	180			150				
11H-Benzo[*b*]fluorine	11BbF		7.6			5.5			
Benzo[*b*]naphtho[*2,1-d*]thiophene	BBNT		0.74			0.59			
5-Methylbenz[*a*]anthracene	5MBA		1.6			1.2			
Benzo[*j*]fluoranthene	BjF		120			95			
11H-Benzo[*a*]fluorine	11BaF		21			26			
4,5-Methanochrysene	4,5MC		34			18			
10-Methylbenzo[*a*]pyrene	10MbA		49			17			
7,12-Dimethylbenz[*a*]anthracene	7,12DbA		3.2			280			
7-Methylbenz[*a*]anthracene	7MbA		18			18			
20-Methylcholanthrene	20MC			68			45		
Ciprofloxacin								0.002	
Genistein								n.a	
Mepanipyrim								0.0001	
Rutaecarpine								0.035	
Protopine									n.a
Bioassay-derived BaP-EQs (ng BaP-EQ g^{-1} dm)		n.a	2800	2600	n.a[b]	1100	170	120	1200
Contribution (%)		n.a	22	2.6	n.a	43	26	0.03	0

[a] Abb: abbreviation.
[b] n.a: not available.

Table S14. Instrumental conditions of HPLC-MS/MS for quantifying novel AhR agonists in sediment samples.

Compounds	MRM transition			
	Precursor Ion	Product Ion	Fragmentor	Collison Energy
Daphnoretin	353	338	165	30
	353	179	165	30
	353	146	165	45
Isorhamnetin	317	217	145	55
	317	203	145	50
	317	153	145	50

Table S15. Instrument and bioassay-derived BaP-EQs and contributions of target compounds to total induced AhR-mediated potencies in sediments obtained from this study and previous studies conducted in South Korea.

Regions	Sites number	Fractions	$BaP\text{-}EQ_{bio}$ (ng g^{-1} dm)	$BaP\text{-}EQ_{chem}$ (ng g^{-1} dm)			Contribution (%)	References
				t-PAHs	e-PAHs	SOs		
Ulsan Bay	4	F2.6	<LOD[a]–420	2.9–220	0.20–14	0.0083–1.1	31–230	Kim et al. (2019)
	4	F2.7	61–1200	0.7–9.3	11–950	0.003–0.025	2.8–26	
Lake Sihwa	4	F2.6	7.5–310	1.2–73	1.2–210	0.014–0.1	2.2–90	Cha et al. (2019)
	4	F2.7	570–1500	7.1–96	10–370	0.005–0.030	2.8–31	
	3	F3.6	29–1810	-	0.004-0.28	-	0.002–0.02	Cha et al. (2021)
	3	F3.7	150–1300	-	<LOD	-	<LOD	
Masan Bay	2	Raw extracts	33000–45000	39–48	-	-	0.11–0.12	Lee et al. (2020)
Yeongil Bay	2	F2.6	340–2300	29–2,000	300–12,300	0.013–0.025	65–98	Gwak et al. (2022)
	2	F2.7	1000–19000	24–2,900	190–2,800	0.010-2.2	20–21	
	2	F2.8	330–1100		2–190		1.7–0.6	
Busan Bay	2	F2.6	<LOD–12	32–59	0.88–1.3	0.0.5–0.75	2400	This study
	2	F2.7	1100–2800	78–152	0.05–130	0.21–0.32	18	
	2	F2.8	170–2500	-	0.06–0.08	-	0.0032	
	2	F3.6	<LOD–120	-	0.35	-	<LOD–0.29	
	2	F3.7	<LOD–1200	-	-	-	<LOD	

[a] <LOD: Below detection limits.

Supplementary Figure

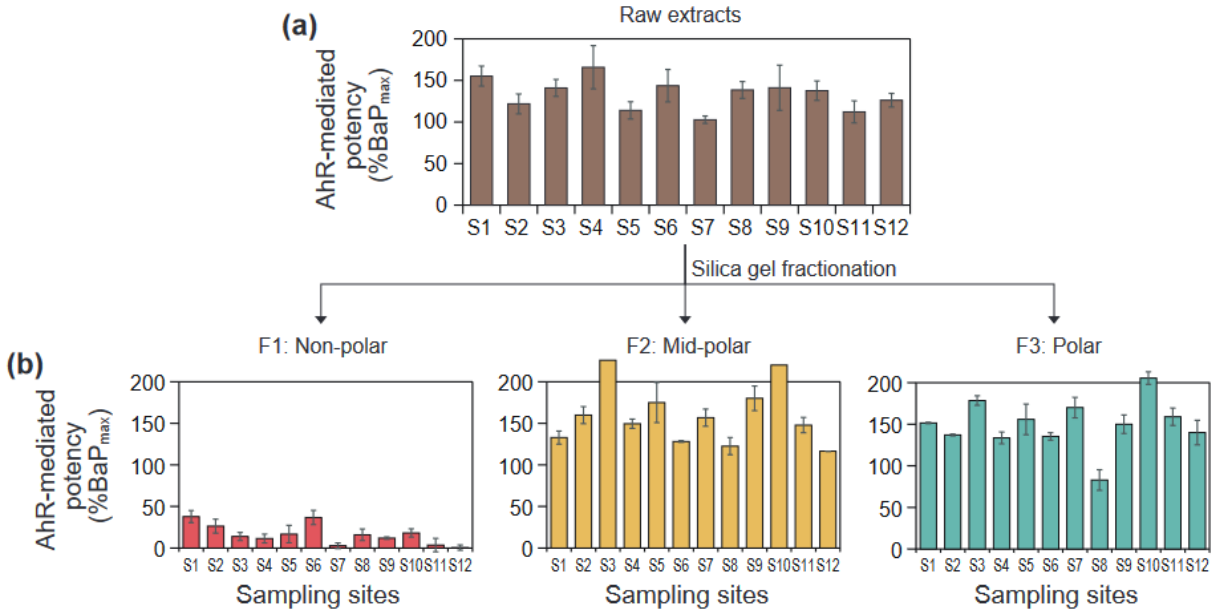

Fig. S1. AhR-mediated potencies in sediments of **(a)** raw extracts and **(b)** silica gel fractions (F1: non-polar; F2: mid-polar; and F3: polar) (error bar: mean ± SD, n = 3).

References

Cha, J., Hong, S., Kim, J., Lee, J., Yoon, S.J., Lee, S., Moon, H.B., Shin, K.H., Hur, J., Giesy, J.P., Khim, J.S., 2019. Major AhR-active chemicals in sediments of Lake Sihwa, South Korea: application of effect-directed analysis combined with full-scan screening analysis. Environ. Int. 133, 105199. https://doi.org/10.1016/j.envint.2019.105199.

Cha, J., Hong, S., Lee, J., Gwak, J., Kim, M., Kim, T., Hur, J., Giesy, J.P., Khim, J.S., 2021. Novel polar AhR-active chemicals detected in sediments of an industrial area using effect-directed analysis based on in vitro bioassays with full-scan high resolution mass spectrometric screening. Sci. Total Environ. 779, 146566. https://doi.org/10.1016/j.scitotenv.2021.146566.

Hong, S., Lee, J., Lee, C., Yoon, S. J., Jeon, S., Kwon, B.O., Lee, J.H., Giesy, J.P., Khim, J.S., 2016. Are styrene oligomers in coastal sediments of an industrial area aryl hydrocarbon-receptor agonists? Environ. Pollut. 213, 913-921. https://doi.org/10.1016/j.envpol.2016.03.025.

Kim, J., Hong, S., Cha, J., Lee, J., Kim, T., Lee, S., Moon, H.B., Shin, K.H., Hur, J., Lee, J.S., Giesy, J.P., Khim, J.S., 2019. Newly identified AhR-active compounds in the sediments of an industrial area using effect-directed analysis. Environ. Sci. Technol. 53, 10043–10052. https://doi.org/10.1021/acs.est.9b02166.

Lee, J., Hong, S., Kim, T., Lee, C., An, S.A., Kwon, B.O., Lee, S., Moon, H.B., Giesy, J.P., Khim, J.S., 2020. Multiple bioassays and targeted and nontargeted analyses to characterize potential toxicological effects associated with sediments of Masan Bay: focusing on AhR-mediated potency. Environ. Sci. Technol. 54, 4443–4454. https://doi.org/10.1021/acs.est.9b07390.

Gwak, J., Cha, J., Lee, J., Kim,Y., An, S.A., Lee, S., Moon, H.-B., Hur, J., Giesy, J.P, Hong, S., Khim, J.S., 2022. Effect-directed identification of novel aryl hydrocarbon receptor-active aromatic compounds in coastal sediments collected from a highly industrialized area. Sci. Total Environ. 803,149969. https://doi.org/10.1016/j.scitotenv.2021.149.